INTERNATIONAL ATOMIC ENERGY AGENCY

9th INTERNATIONAL CONFERENCE ON PLASMA PHYSICS AND CONTROLLED NUCLEAR FUSION RESEARCH

Baltimore, USA, 1–8 September 1982

IAEA-CN-41/ E-1-1

32

TOKAMAK REACTOR STUDIES: STUDIES OF DT DEMONSTRATION REACTORS AND DD REACTORS

C. Baker, M. Abdou, C. Boley, J. Brooks, R. Clemmer, D. Ehst, K. Evans, P. Finn, Y. Gohar, J. Jung, R. Mattas, B. Misra, D. Smith, H. Stevens, L. Turner, and R. Wehrle
Argonne National Laboratory
Argonne, Illinois 60439, USA

G. D. Morgan, C. Trachsel, L. Waganer, and D. DeFreece
McDonnell Douglas Astronautics Company
St. Louis, Missouri 63166, USA

F. Perkins, N. Fisch, D. Hwang, D. Ignat, S. Jardin, C. Karney, K. Ling, D. Mikkelsen, C. Singer, and Y. Sun
Princeton Plasma Physics Laboratory
Princeton, New Jersey 08544, USA

D. Baxter, R. Byrne, A. Dabiri, D. Dobrott, J. Glancy, W. Hagan, J. McBride, and S. Tamor
Science Applications, Inc.
La Jolla, California 92038, USA

K. Berry
The Ralph M. Parsons Company
Pasadena, California 91125, USA

R. McGrath
The Pennsylvania State University
University Park, Pennsylvania 16802, USA

IAEA-CN-41/E-1-1

TOKAMAK REACTOR STUDIES: STUDIES OF DT DEMONSTRATION REACTORS AND DD REACTORS

Abstract

This paper summarizes several issues related to the application of tokamak devices as fusion power reactors. Most of this work deals with DT plasmas and tokamak devices sized to be representative of a fusion demonstration (DEMO) power reactor. Key DEMO issues include current drive, impurity control, and tritium breeding blankets. Current drive topics include startup and steady-state plasma current maintenance by a variety of techniques. Issues related to DD-fueled reactors are also discussed, including effects of synchrotron radiation, nuclear elastic scattering, and features of DD reactors compared to DT reactors.

1. TOKAMAK DT DEMONSTRATION REACTOR

The objectives of the DEMO are to demonstrate a level of performance in a power plant which extrapolates to commercial plants; a system availability which extrapolates to commercial plant values; a complete tritium breeding, power-producing blanket; and safe operation of a prototype power plant.

Satisfying these objectives requires that the DEMO design features and performance be as close as practicable to those of a commercial reactor. Two constraints must be recognized: the DEMO capital cost should be minimized and the performance requirements should be consistent with a fusion R&D plan which realistically accounts for financial and time-schedule considerations. The cost constraint primarily affects the selection of the DEMO size (physical size and thermal power). The fusion R&D plan constraint primarily influences the selection of the availability goal for the DEMO.

For given technological (e.g., maximum magnetic field) and physics (e.g., maximum beta) constraints, the minimum size that can be considered for the DEMO is defined primarily by ignition requirements. For a maximum magnetic field, B_m = 10 T, and plasma elongation, κ = 1.6, the major and minor radii are in the range of R = 5.0-5.2 m and a = 1.2-1.3 m. For the DEMO, we selected B_m = 10 T in order to reduce the design risks and cost associated with higher fields. Furthermore, results from STARFIRE [1], INTOR [2], and FED [3] indicate that κ = 1.6 is a reasonable compromise between the benefits (higher beta) of increased elongation and the equilibrium field (EF) coil requirements, particularly when all these coils are placed outside the TF coils. The optimum blanket/shield thickness for a wide range of DEMO conditions was previously found to be Δ_{BS}^{i} = 1.2 m. [4]

The size of FED and INTOR is adequate for the DEMO except for the low value of the neutron wall load, W_n, which will likely be $W_n = 3.0\text{-}4.0$ MW/m^2 for commercial tokamaks. A higher wall load can be achieved only by increasing the power density in the plasma and/or by increasing the physical size of the device. Both will increase the capital cost of the DEMO. In general, better economics is obtainable for fusion reactors by increasing the plasma power density rather than increasing the reactor physical size. In this study, we assume that some improvement in beta beyond that predicted for FED and INTOR will be achievable in the DEMO. Therefore, $\beta = 0.075$ has been selected as the goal.

For fusion reactors to be economically competitive, a plant availability of 65-75% must be achieved. In the DEMO study, the importance of the availability factor has been recognized in two ways. First, a plant availability goal of 50% was adopted. Given that FED and INTOR are planned for ~ 10-20% availability, this DEMO goal provides an ambitious target for technology development. Second, every effort is being taken to incorporate design features that enhance the probability of achieving high availability. The most important design feature selected to maximize component lifetime and reliability in the DEMO is steady-state plasma operation. By eliminating cyclic loads, steady-state operation enhances the reliability of components such as the first wall, blanket, limiters, divertors, and magnets. In addition, the frequency of plasma disruption is reduced.

Component lifetime and reliability are also enhanced in the DEMO by locating key components away from the harsh radiation environment. All the superconducting EF coils are located outside the TF coils except for some small copper control coils. Other features include locating the vacuum boundary at the shield with all mechanical seals at the exterior and selecting only eight TF coils with the use of one blanket/shield sector per TF coil.

The major parameters for the DEMO, along with the STARFIRE parameters for comparison, are listed in Table I. A cross section of the DEMO reactor is shown in Fig. 1.

2. CURRENT DRIVE IN TOKAMAKS

A simulation code has been developed to address current build-up problems. Principal features include: (1) a very fast plasma equilibrium algorithm based on a spectral representation [5]; (2) self-consistent flux linkages between the driven external coils, eddy currents in conducting shells (which are required for electromagnetic shielding from disruptions), and the plasma; (3) constant q-profile; and (4) variable toroidal flux within the plasma. Features (3) and (4) depart from the usual ideal MHD assumptions and model internal current profile relaxation processes. Stated simply, if current relaxation processes fix the q-profile of a tokamak, then the plasma current will be directly proportional to the toroidal flux contained in the plasma.

TABLE I. Major Design Parameters for STARFIRE and DEMO

	STARFIRE	DEMO
Fusion Power, MW	3500	1060
Thermal Power, MW	4000	1290
Net Electrical Power, MW	1200	350
Overall Availability, %	75	50
Average Neutron Wall Load, MW/m^2	3.6	2.1
Major Radius, m	7.0	5.2
Plasma Half-Width, m	1.94	1.3
Plasma Elongation, (b/a)	1.6	1.6
Plasma Current, MA	10.1	8.7
Average Toroidal Beta, %	6.7	7.5
Maximum Toroidal Field, T	11.1	10.0
No. of TF Coils	12	8
Plasma Burn Mode	Continuous	Continuous
Current Drive Method	RF (LH)	REB
First Wall/Blanket Structural Material	PCA[a] (SS)	PCA[a]
First Wall/Blanket Coolant	Water	Water
Tritium Breeding Medium	Solid Breeder ($LiAlO_2$)	Solid Breeder (LiO_2)

[a]Primary Candidate Alloy (PCA), an advanced austenitic stainless steel

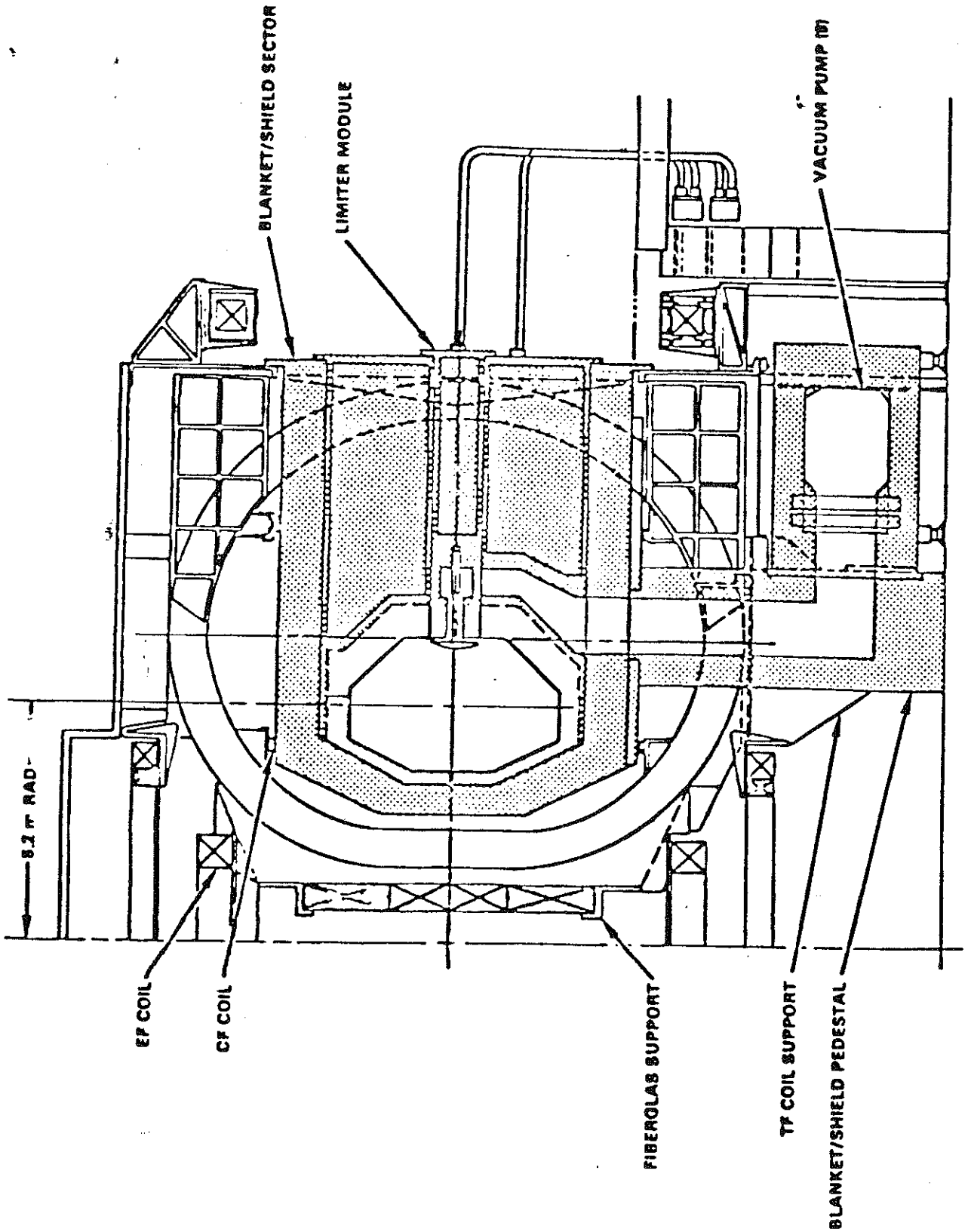

FIG. 1. DEMO reference design.

Because the plasma current must be consistent with flux linkages involving external coils, the toroidal flux within the plasma and, hence, the plasma size will increase as the current builds up. Initial runs have shown that a stable axisymmetric plasma equilibrium can be maintained for an order-of-magnitude increase in plasma current with a relatively simple poloidal field coil configuration.

For neutral-beam-driven steady-state operation, we have used a reactor model which includes beam-driven current physics, plasma power balance, electrical power flows, and reactor system costs to determine the optimum plasma temperatures and neutral beam energy. The optimum temperatures for INTOR are $\bar{T}_e$ = 12-15 keV and $\bar{T}_i$ = 17-21 keV. [6] The net electrical output of the reactor rises rapidly with deuterium beam energy until it saturates for $E_{NB} > 1$ MeV. The electrical efficiency of the neutral beam system, η_{NB}, also strongly affects the electrical output, which falls rapidly for $\eta_{NB} < 0.6$. We find that 100 MW of 2 MeV D^o is required to drive I = 6.4 MA in INTOR.

Current maintenance by electron TTMP damping of fast Alfven waves is crucially dependent on the weak TTMP absorption dominating over competitive processes such as absorption caused by cyclotron (or perpendicular Landau) damping on α-particles. For a Maxwellian, the attenuation from TTMP on one pass through the plasma is $e^{-\Delta}$, where

$$\Delta = \frac{\sqrt{\pi}\, a}{\lambda_\parallel} \left(\frac{M_i}{m_e}\right)^{1/2} \left(\beta_{e,o}\right)^{3/2} x^2 e^{-x^2} \approx 2x^2 e^{-x^2}.$$

Here $x = (\omega/k_\parallel)(m/2T_e)^{1/2}$ and $\beta_{e,o} = 0.06$ is the central electron β. If we wish to achieve 10-pass absorption ($\Delta \approx 10^{-1}$), then $x^2 = 4.5$ and $k_\parallel = 2.5$, given $T_{e,o} = 10$ keV. Damping on any ion species can be avoided if the frequency ω is chosen to lie in the range $\Omega_{He^3} < \omega < \Omega_p$. For $B_T = 6$ T, we obtain $\upsilon = 75$ MHz and $\lambda_\parallel = 1.6$ m. The inequality on the frequency can be satisfied provided the aspect ratio exceeds 5. For other choices of frequency, calculations show damping on fusion α-particles to be competitive with electron TTMP. The fast wave antenna will be a phased array of reentrant waveguides. [7] The long parallel wavelength implies that only modest evanescent decay will occur in the plasma scrapeoff region. The weak damping assures that the fast wave energy will be deposited in the plasma center where the electron temperature is high. The principal disadvantage is that the energy of the current-carrying electrons is low (≈ 50 keV) which results in low current drive efficiency because of the drag on these electrons. Thus, fast wave current drive also benefits from high-temperature (low-density) operating points.

Pulsed power injection provides reductions in the time-averaged power, $\langle P_d \rangle$, requirement compared to purely CW current

drive when combined with density or resistivity oscillations. Large beam-driven resistivity oscillations may occur during repetitive injection of a relativistic electron beam (REB), and, ideally, $\langle P_d \rangle$ approaches the ohmic limit, I^2R. [8] Net power production in the DEMO is compared in Fig. 2 for a pulsed REB, CW neutral injection, and the CW fast wave. [9] The REB technique has the advantage that plasma density, temperature, and current remain nearly static, but REB radial penetration is uncertain.

If density and temperature are permitted to oscillate, then $\langle P_d \rangle$ can also be reduced for neutral beams. A reactor similar to DEMO can be driven optimally with only 60 MW of beam injectors at much lower energies than required for strictly CW operation. [10] Present neutral beam efficiencies of 20% or more allow net power production around 560 MW for 400 keV beams, 500 MW for 200 keV beams, and 240 MW for 120 keV beams. The higher energy beams would be required to lower the injection duty cycle to about 5 seconds out of every minute of operation.

Lower hybrid waves [11] can likewise provide current maintenance if cyclic density and temperature operation is used. [12] As with neutral beams, the current drive power is applied during a low-density period when the inherent current drive efficiency is higher. Also, the lower density raises the phase velocity at which mode conversion occurs, thereby permitting the use of higher phase velocity waves which not only increase the current drive efficiency but also avoid electron Landau damping in the plasma periphery. Overall, there is about a tenfold reduction in $\langle P_d \rangle$, and the peak power requirements are reduced by a factor of five.

3. IMPURITY CONTROL ENGINEERING IN DEMO

Impurity control is provided by a pumped limiter system which is located at the outer midplane of the reactor (see Fig. 1). The outer midplane was selected because of the increased accessibility, reduced potential for disruption damage, and reduced magnetic coil sizes offered by that location. Since the limiter is anticipated to have a lower lifetime than the first wall and blanket, the limiter is designed to be replaced separately as part of the limiter/blanket module. During normal operation, ~ 5% of the particles escaping from the plasma enter the channels behind the limiter and are neutralized. The neutralized particles then enter the vacuum ducts and travel down to the vacuum pumps located below the reactor.

The limiter consists of a double-bladed structural core, which provides support and contains the coolant passages, upon which a surface material is bonded. The limiter is shaped to produce a roughly uniform heat load of 2.0 MW/m^2 to the surface exposed to the plasma. The maximum heat load to the leading edges is ~ 1 MW/m^2. The total power handled by the limiter is about 100 MW, which is about 50% of the α-particle power. The remaining energy is radiated to the first wall. The overall length of the

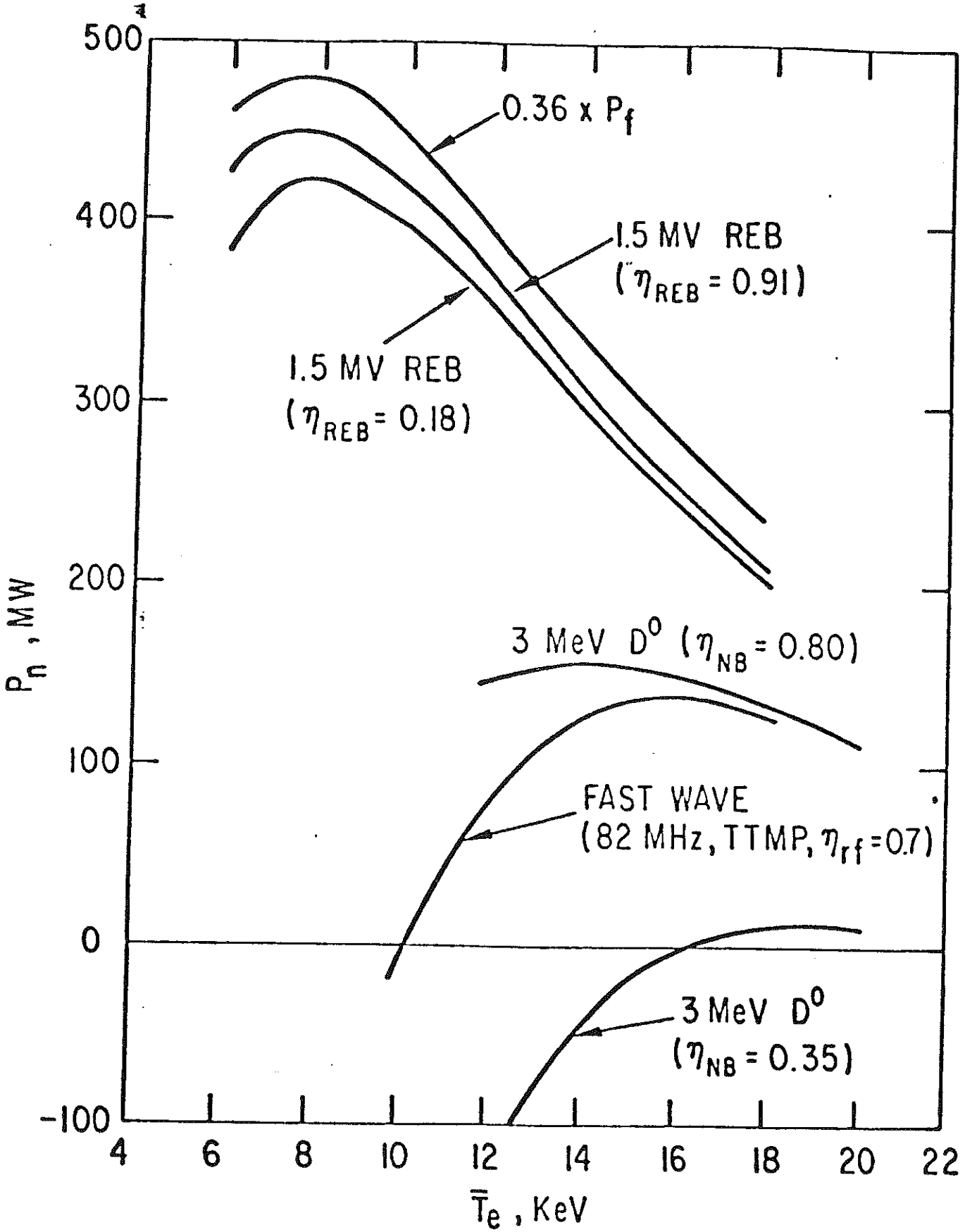

FIG. 2. Gross power (0.36 x P_f) for DEMO and net electric power for three driver candidates: continuous neutral injection (3 MeV D^0); continuous fast wave (82 MHz); and pulsed REB (1.5 MeV, 4 MJ per pulse). $\bar{T}_e$ is varied with $\beta \equiv 8\%$; $P_n = (0.36 \times P_f) - 22 - (P_d/\eta_d)$, in MW.

limiter is 1.5 m, and the width of individual limiter segments is 0.5 m. The segments are placed together to form a continuous belt limiter in the toroidal direction. Short limiter segments were selected to reduce magnetic torques during disruptions, reduce the voltage drop between segments during disruptions, and eliminate the need for incorporating toroidal curvature in the limiter blades.

Two surface materials are required to achieve an extended limiter lifetime. Beryllium and tantalum have been selected as the front surface coating material and leading edge coating material, respectively. Sputtering/redeposition calculations indicate a net erosion rate of ~ 0.7 cm/y at 50% duty factor for the Be and zero for tantalum at the leading edge. For comparison, the erosion rate for Be at the leading edge would be ~ 15 cm/y. No tantalum impurities are expected to enter the plasma since the typical mean free path of a sputtered tantalum particle is only ~ 0.1 mm before it is ionized and redeposited. The major concern with the use of beryllium is the predicted large (100-200 μm) melt layer formation during a disruption. Steady-state operation should alleviate much of this problem, however. The major concern with the use of tantalum is that the self-sputtering coefficient exceeds unity at particle energies greater than ~ 700 eV, leading to a runaway sputtering condition. Tantalum is predicted to ionize to the +4 charge state after it is sputtered, and, therefore, the tantalum ions are expected to acquire an energy of ~ 12 T_e through the limiter sheath potential. In order to keep the energy below 700 eV, the plasma temperature at the leading edge should be less than ~ 50 eV, a condition which is satisfied for edge temperatures at the limiter tip of about 100 eV.

4. DEMO BLANKET DESIGN

The DEMO study focused on definition of materials and design issues for blankets using solid Li_2O breeder and liquid Li-Pb breeder blanket concepts. For the reference choice of the Li_2O concept, pressurized water was selected for the first wall and blanket coolant. An advanced austenitic stainless steel similar to Type 316 was selected as the structural material. Its mechanical properties and radiation damage resistance are considered acceptable for reasonable lifetimes (~ 10 years) at projected operating temperatures.

Tritium recovery is considered to be the key feasibility issue regarding the viability of Li_2O as a tritium breeder material. An Li_2O microstructure with small grain size (< 1 μm) and a bimodal pore distribution is recommended. The limited operating temperature range projected for Li_2O (410-660°C) and the low thermal conductivity result in difficult design problems. In the absence of radiation effects, the blanket tritium inventory is predicted to be < 50 g. However, radiation effects are expected to substantially increase this value.

The first wall and blanket of the Li_2O blanket are integrated mechanically and structurally into modules. The first wall is a beryllium-clad corrugated panel. The breeder and first wall are cooled by high-pressure (11.0 MPa), high-temperature (260°C inlet, 300°C outlet) water. The breeder coolant is contained in small-diameter tubes connected to manifolds at the rear of the blanket. The breeder is fabricated at 70% of theoretical density with bimodal porosity to enhance tritium release. Helium purge gas (~ 1 atm) flows through 2-mm diameter holes in the breeder to remove tritium.

Liquid Li-Pb alloys have several attractive properties. The neutron multiplication by the lead provides excellent tritium breeding performance, and the neutron attenuation properties of the alloy are attractive for radiation shielding. The 17Li-83Pb eutectic alloy was selected as the reference liquid breeder.

An important initial consideration for the blanket design is whether to use Li-Pb as both breeder and coolant or to use a separate gas or liquid coolant. Helium, pressurized water, and liquid sodium were considered as coolants. Sodium is considered at present to be the best separate coolant, primarily because of its good thermal-hydraulic characteristics, its low reactivity with Li-Pb, and its potential to serve as a tritium-recovery medium without requiring Li-Pb circulation. However, reactivity of sodium with water and air is a safety concern. Vanadium alloys or ferritic steels appear to be appropriate choices for the structural material.

Because of the low solubility of tritium in 17Li-83Pb, fairly high tritium pressures (about 1 Pa) are required for acceptable flowrates if Li-Pb is used as the tritium recovery fluid. The molten salt extraction process is considered the most appropriate method for direct recovery of tritium from Li-Pb. For a sodium coolant, permeation rates into the sodium appear to be sufficient to use the sodium as the tritium recovery fluid.

Compatibility with the structural material is a key feasibility question for the Li-Pb blanket. Ferritic steels without nickel should be more resistant to mass transfer effects than austenitic steels at operating temperatures (> 400°C). However, low-temperature (~ 350°C) liquid metal embrittlement phenomena are of concern.

5. DD TOKAMAK STUDIES

This section describes results of DD tokamak studies. These studies emphasize treatment of the physics processes that are important for modeling the high-temperature regime of DD reactor operation. For example, synchrotron radiation is an important consideration. Although the emission rate is large, reabsorption of energy reflected from the walls is sufficient to bring the radiation loss down to tolerable levels. A synchrotron radiation

transport code, CYTRAN [13], is used to calculate the power absorbed or emitted in a flux shell due to all the other shells in the plasma. Absorption coefficients are obtained from an updated OPAKE code. [14] The synchrotron power contribution obtained from CYTRAN was used in the one and one-half dimensional DD reactor transport code DDMAK to: (1) self-consistently determine the total energy loss by radiation and its dependence on wall reflectivity, (2) compare temperature profiles with those obtained from locally applied formulas such as that of Trubnikov [15], and (3) estimate the relative importance of radiation and thermal conduction in determining the temperature profile. We find that the Trubnikov model provides a good estimate of the net radiation loss. We also find that the standard model can be in error in predicting temperature profiles. Self-consistent profiles using CYTRAN are significantly flatter near the center. The profile shapes may be as sensitive to radiation transport as to thermal conduction.

Nuclear elastic scattering (NES) effects were also studied using DDMAK. [16] When NES is included in the slowdown model, the fraction of the slowdown energy being deposited in the background ions is enhanced numerically at the expense of the slowdown energy deposited in the electrons. In a DD reactor, only the 14.7 MeV protons, created by the D-^{3}He reactions, have sufficiently long slowdown time to be significantly affected by this process. For temperatures < 60 keV, the ion energy enhancement is $< 10\%$. Ion and electron steady-state temperature profiles with and without the NES effects are calculated and are nearly identical. We conclude from these studies that NES is not a quantitatively important mechanism in DD tokamaks at temperatures in the neighborhood of $\sim$ 50-60 keV.

High beta will be a requirement if a DD tokamak is to be a viable reactor. Recent theoretical results on non-linear saturation of resistive ballooning modes [17] indicate a fluctuation spectrum that is similar to that observed in experiments. These results suggest that if present day experiments are limited by resistive ballooning modes, this limitation may not be of concern for reactor scale tokamaks. Previous work [18] indicates a possible stable β enhancement of 40%. The most favorable characteristics appear to be equilibria with low shear in regions of large pressure gradients.

A design of a catalyzed DD tokamak reactor, called WILDCAT, has been completed. The lower reaction rates of the DD fuel cycle result in a device that is larger in major radius (8.6 vs. 7.0 m), has higher toroidal field (14.4 vs. 11.1 T), and operates at a higher beta (11% vs 7%) than STARFIRE. The DD reactor must operate at a higher average plasma temperature ($\sim$ 30 keV) and must have an order of magnitude fewer impurities to achieve ignition. On the other hand, there are two major advantages of DD operation: issues and problems regarding tritium breeding are eliminated and tritium inventories, handling, and releases are reduced nearly two orders of magnitude.

Designs for both a steady-state (with an Alfven-wave current drive) and pulsed version have been made. The pulsed version is about 25% more expensive because of the power supplies and the required thermal storage system. Since WILDCAT does not have to breed tritium, the blanket/shield can be optimized to have a thinner inboard extent (82 vs. 120 cm for STARFIRE), leading to more efficient use of the toroidal field, and to have increased neutron energy multiplication in the blanket (2.02 vs. 1.14 for STARFIRE).

REFERENCES

[1] BAKER, C. C., et al., STARFIRE - A Commercial Tokamak Fusion Power Plant Study, Argonne National Laboratory Rep. ANL/FPP-80-1 (1980); ABDOU, M. A., et al., "STARFIRE - a conceptual design of a commercial tokamak power plant," Plasma Physics and Controlled Nuclear Fusion Research 1980 (Proc. 8th Conf. Brussels, 1980) Vol. II, IAEA, Vienna (1981) 119.

[2] The Fusion Engineering Device, U. S. Department of Energy Rep. DOE/TIC-1160 (1981).

[3] U. S. INTOR Conceptual Design, Phase I, USA-INTOR/81-1 (1981).

[4] ABDOU, M. A., Radiation considerations for superconducting fusion magnets, J. Nucl. Mater. 72 (1978) 147.

[5] LING, K. M., JARDIN, S. C., Free boundary-problem in two-dimensional tokamak plasma equilibrium, Bull. Am. Phys. Soc. 26 (1981) 957.

[6] MIKKELSEN, D. R., SINGER, C. E., Optimization of Steady-State Beam-Driven Tokamak Reactors, Princeton Plasma Physics Laboratory Rep. PPPL-1929 (1982).

[7] PERKINS, F. W., "An ICRF antenna," 4th Top. Conf. on Radio Frequency Plasma Heating, Austin, Texas (1981) B13.

[8] EHST, D. A., "Driver options for steady-state tokamak reactors," 9th Symp. on Engineering Problems of Fusion Research, Chicago, Illinois (1981) Vol. I, 708.

[9] ABDOU, M. A., et al., A Demonstration Tokamak Power Plant Study - Interim Report, Argonne National Laboratory Rep. ANL/FPP/TM-154 (1982).

[10] SINGER, C. E., MIKKELSEN, D. R., Continuous Tokamak Operation with an Internal Transformer, Princeton Plasma Physics Laboratory Rep. PPPL-1948 (1982).

[11] Princeton PLT Group, this conference; YAMAMOTO, T., et al., Phys. Rev. Lett. 45 (1980) 716; LUCKHARDT, S. L., et al., Phys. Rev. Lett. 48 (1982) 152.

[12] FISCH, N. J., "Current generation in toroidal plasma," 3rd Joint Grenoble-Varenna International Symp. on Heating in Toroidal Plasma, Grenoble, France (1982) Vol. III.

[13] TAMOR, S., A Simple Fast Routine for Computation of Energy Transport by Synchrotron Radiation in Tokamaks and Similar Geometries, Science Applications, Inc. Rep. SAI-023-81-189LJ/LAPS-72 (1981).

[14] TAMOR, S., Nucl. Fusion 18 229 (1978).

[15] TRUBNIKOV, B. A., "Universal coefficients for synchrotron emission from plasma configurations," Reviews of Plasma Physics, Vol. 7 (LEONTOVICH, M. A., Ed.), Consultants Bureau, New York (1979) and JETP 16 1 (1972).

[16] BAXTER, D. C., BYRNE, R. N., GALAMBOS, J., STROUD, P., GILLIGAN, J., "Nuclear elastic scattering in cat-D tokamaks," submitted to Nuclear Technology/Fusion (1982).

[17] STRICKLER, D. J., PENG, Y-K. M., LEE, D. K., Pressure Profile Effects on the Ballooning Mode Stability of the FED Tokamak, Oak Ridge National Laboratory Rep. ORNL/TM-8040 (1982).

[18] CARRERAS, B. A., et al., "Resistive pressure driven modes in high β tokamaks," Paper 2C1, Annual Fusion Theory Sherwood Meeting, Sante Fe, New Mexico (1982).